

ニュートリノ二重ベータ崩壊の機構

岩田順敬（関西大学）

Yoritaka Iwata (Kansai University)

Ref.) **Y. Iwata, N. Shimizu et al. Phys. Rev. Lett. 2016**

J. Terasaki, Y. Iwata, Phys. Rev. C 2019

S. Sarkar, Y. Iwata, P. K. Raina, Phys. Rev. C 2020

Half-life & nuclear matrix element (NME)

$$1/T_{0\nu}(\text{g. s.} \rightarrow \text{g. s.}) = |M^{(0\nu)}|^2 G_{0\nu} g_A^4 \left(\frac{\langle m_\nu \rangle}{m_e} \right)^2$$

半減期

NME

Axial vector current
coupling constant

位相空間因子

m_e : 電子質量

位相空間因子 ← 放出される電子の波動関数

↑
正確な計算が可能

原子核行列要素 ← 原子核の波動関数

↑
近似が不可欠

↓
正確な計算は位相空間因子より難しい

Theoretical methods nuclear matrix element (NME)

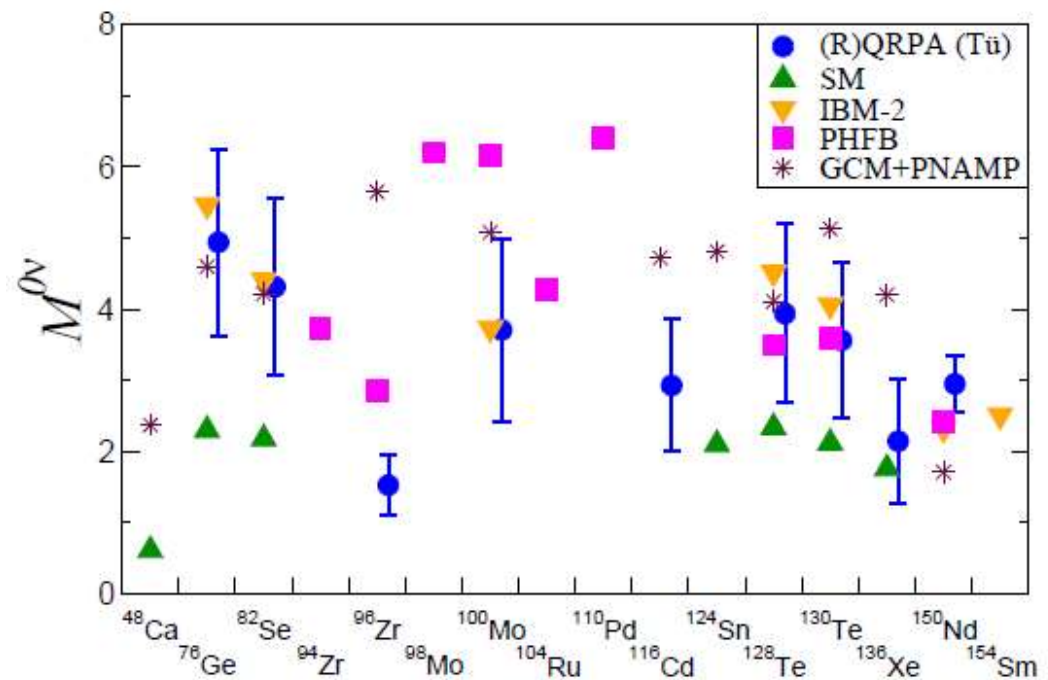
ISM (殻模型計算=相互作用するフェルミオン模型)

IBM (相互作用するボソン模型)

QRPA (準粒子乱雑位相近似)

HFB, EDF (対相関入り平均場計算)

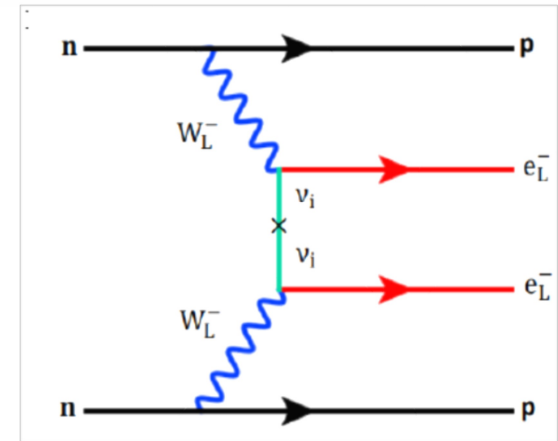
GCM (生成座標の方法)



Feassler, J. Phys. Conf. Ser. 2012.

Contents

- × Shell model research [overview]
- × Shell model calculation for DBD of Ca48
 - Large scale calculation by Tokyo group -
- × Right handed weak boson ?
- × Summary



Recent trend on ISM calculations:

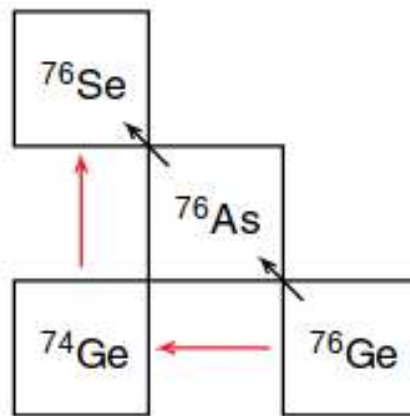
① “more structure” = new paths

PRL 113, 262501 (2014)

PHYSICAL REVIEW LETTERS

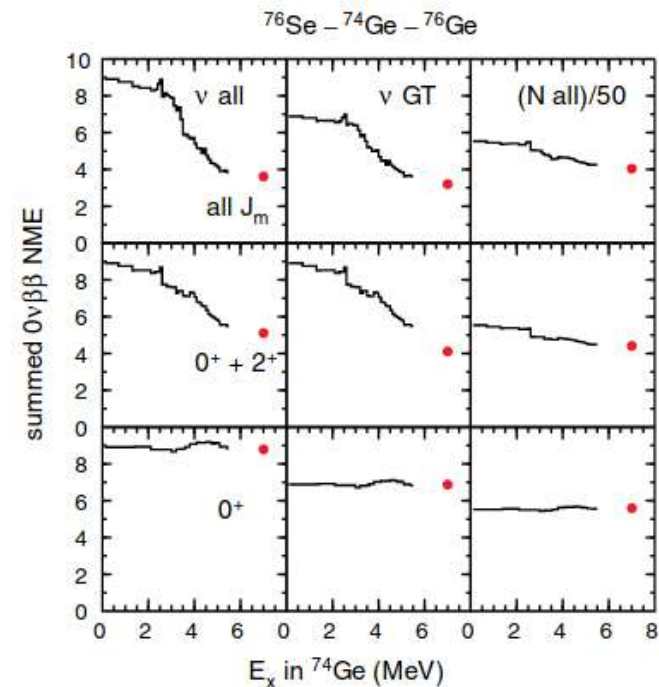
week ending
31 DECEMBER 2014

Nuclear Structure Aspects of Neutrinoless Double- β Decay

B. A. Brown,¹ M. Horoi,² and R. A. Sen'kov^{2,3}¹*Department of Physics and Astronomy and National Superconducting Cyclotron Laboratory,
Michigan State University, East Lansing, Michigan 48824-1321, USA*²*Department of Physics, Central Michigan University, Mount Pleasant, Michigan 48859, USA*³*Department of Natural Sciences, LaGuardia Community College, The City University of New York,
Long Island City, New York 11101, USA*

→ **DGT, 2 ν , 0 ν**
Experiments

At the same time



Recent trend on ISM calculations:

② Hadronic current by EFT

PHYSICAL REVIEW C **98**, 035502 (2018)

Shell model study of using an effective field theory for disentangling several contributions to neutrinoless double- β decay

Mihai Horoi^{*} and Andrei Neacsu[†]

Department of Physics, Central Michigan University, Mount Pleasant, Michigan 48859, USA

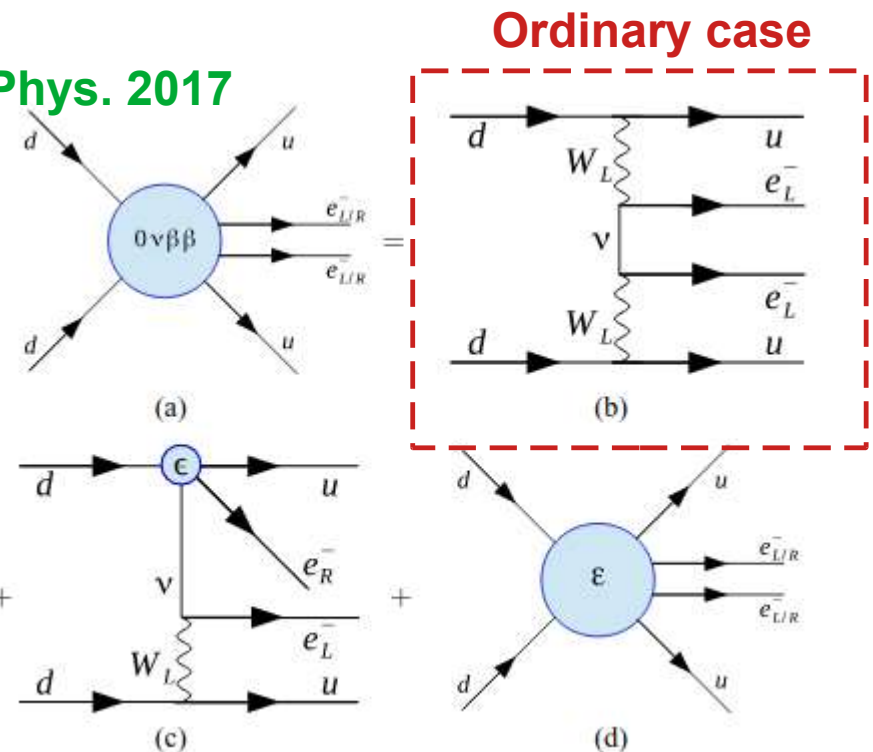
[λ mechanism] see also ... Simkovic et al., Front Phys. 2017

$$[T_{1/2}^{0\nu}]^{-1} = G_{01} g_A^4 |\eta_{0\nu} M_{0\nu} + (\eta_{NR}^L + \eta_{NR}^R) M_{0N} + \eta_{\bar{q}} M_{\bar{q}} + \eta_{\lambda'} M_{\lambda'} + \eta_{\lambda} X_{\lambda} + \eta_{\eta} X_{\eta}|^2.$$

the left-right symmetric model
with R-parity-violating SUSY model

→ for contributions of

\mathbf{V}_L , \mathbf{V}_R , \mathbf{W}_L , \mathbf{W}_R



Recent trend on ISM+ calculations:

③ Ab-initio (IMSRG usable for ISM)

PHYSICAL REVIEW LETTERS **124**, 232501 (2020)

Ab Initio Treatment of Collective Correlations and the Neutrinoless Double Beta Decay of ^{48}Ca

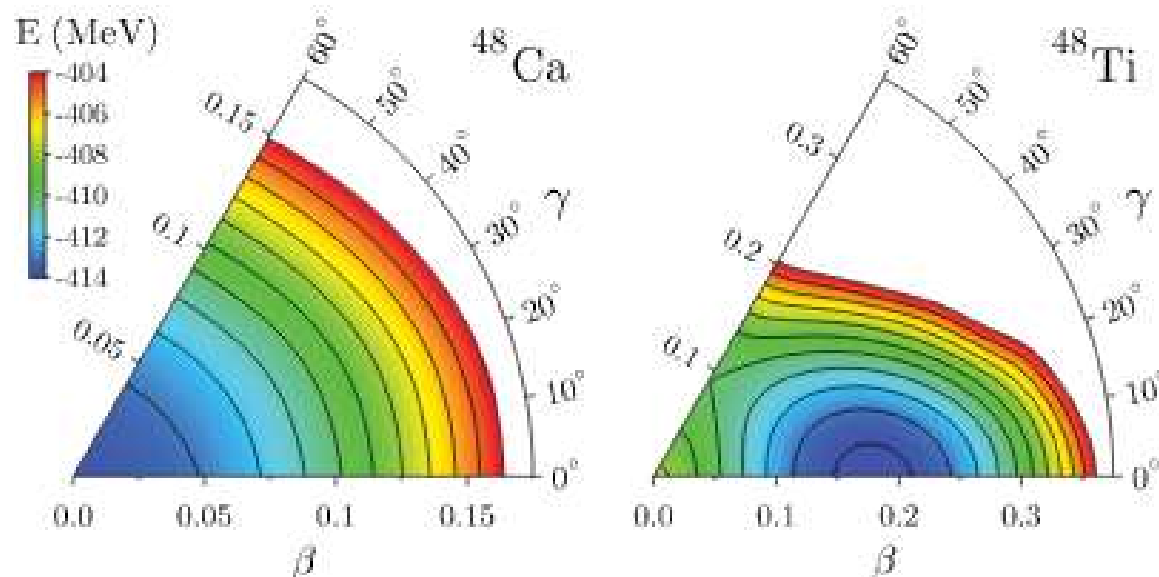
J. M. Yao^{1,*}, B. Bally^{2,†}, J. Engel^{2,‡}, R. Wirth^{1,§}, T. R. Rodríguez^{3,||} and H. Hergert^{1,4,¶}

¹Facility for Rare Isotope Beams, Michigan State University, East Lansing, Michigan 48824-1321, USA

²Department of Physics and Astronomy, University of North Carolina, Chapel Hill, North Carolina 27516-3255, USA

³Departamento de Física Teórica y Centro de Investigación Avanzada en Física Fundamental,
Universidad Autónoma de Madrid, E-28049 Madrid, Spain

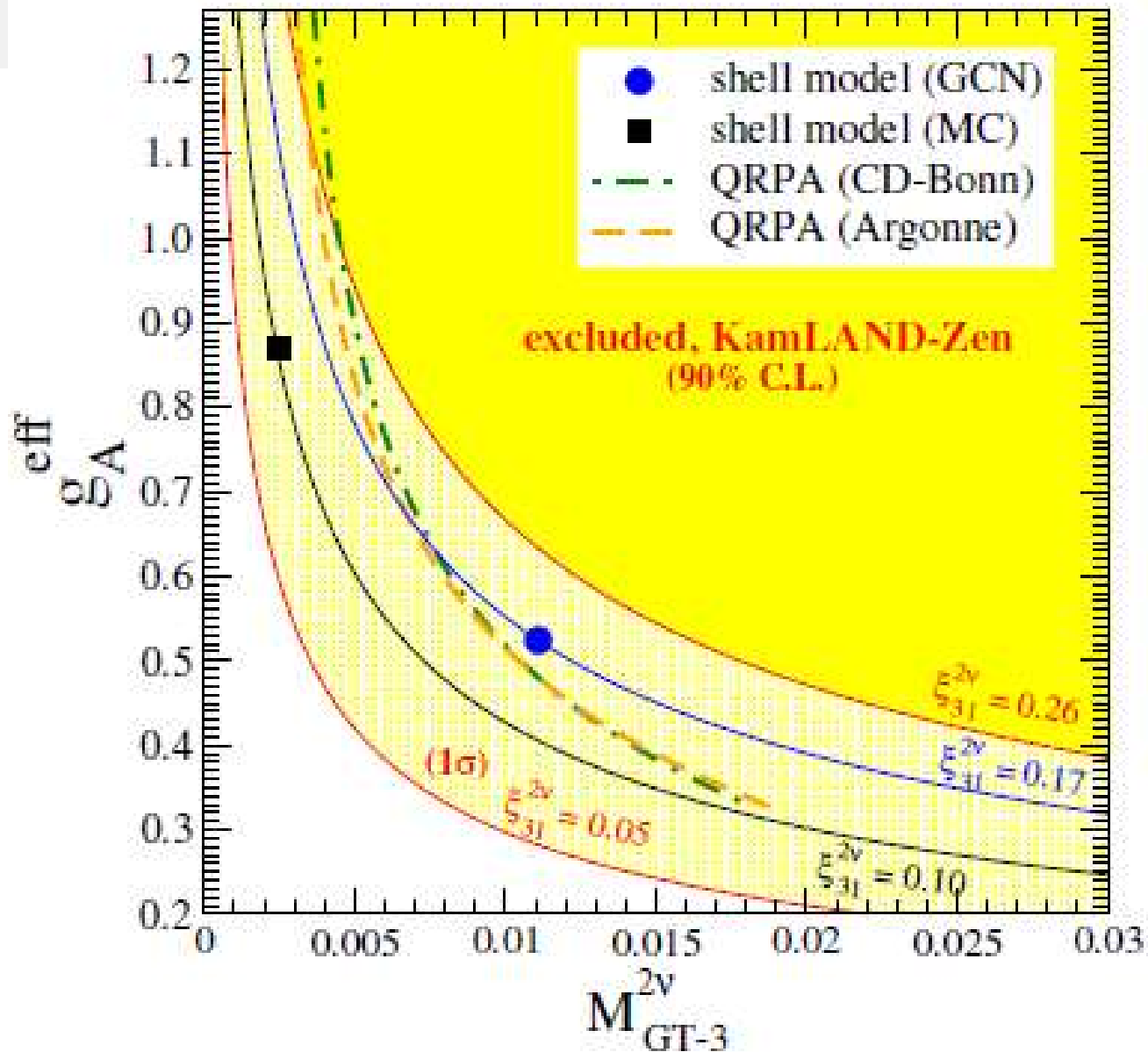
⁴Department of Physics & Astronomy, Michigan State University, East Lansing, Michigan 48824-1321, USA



$$M^{0\nu} = 0.61$$

GCM

Recent trend on NME calculations:



Based on
2ν experiment

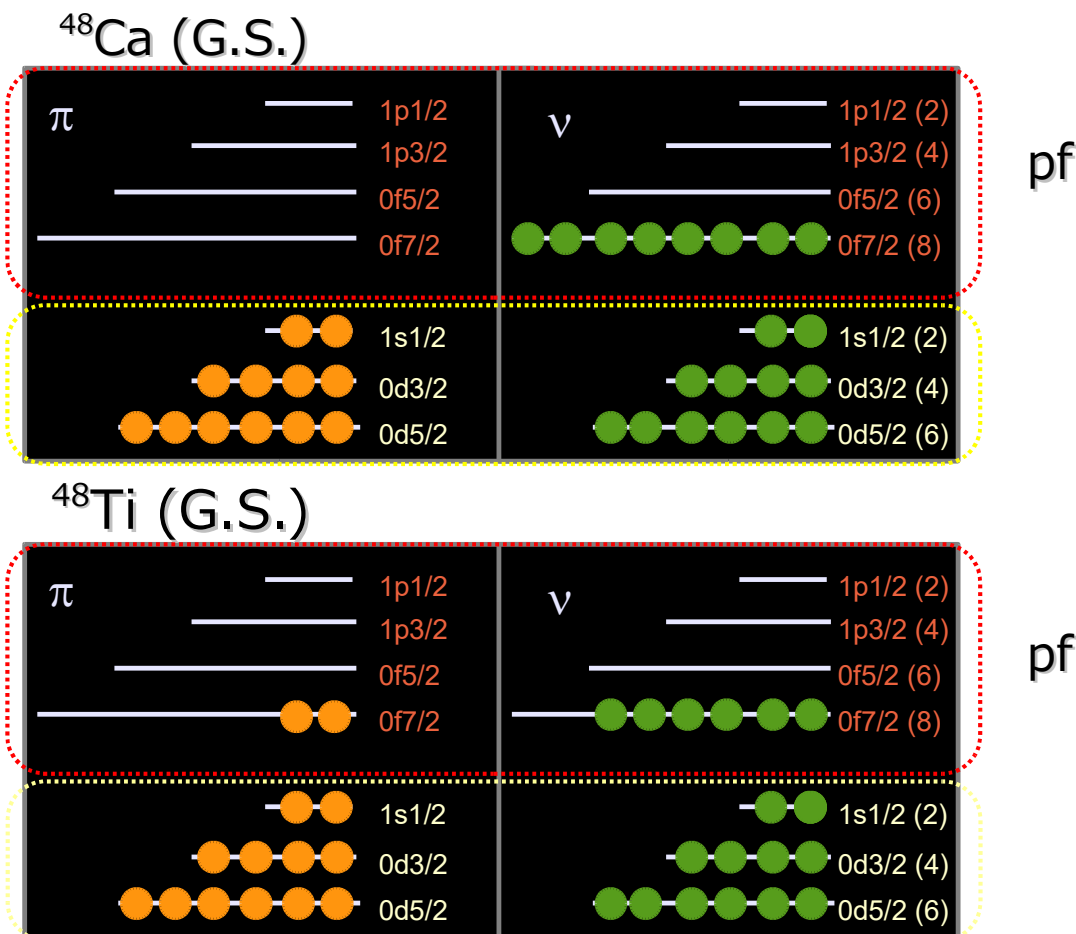
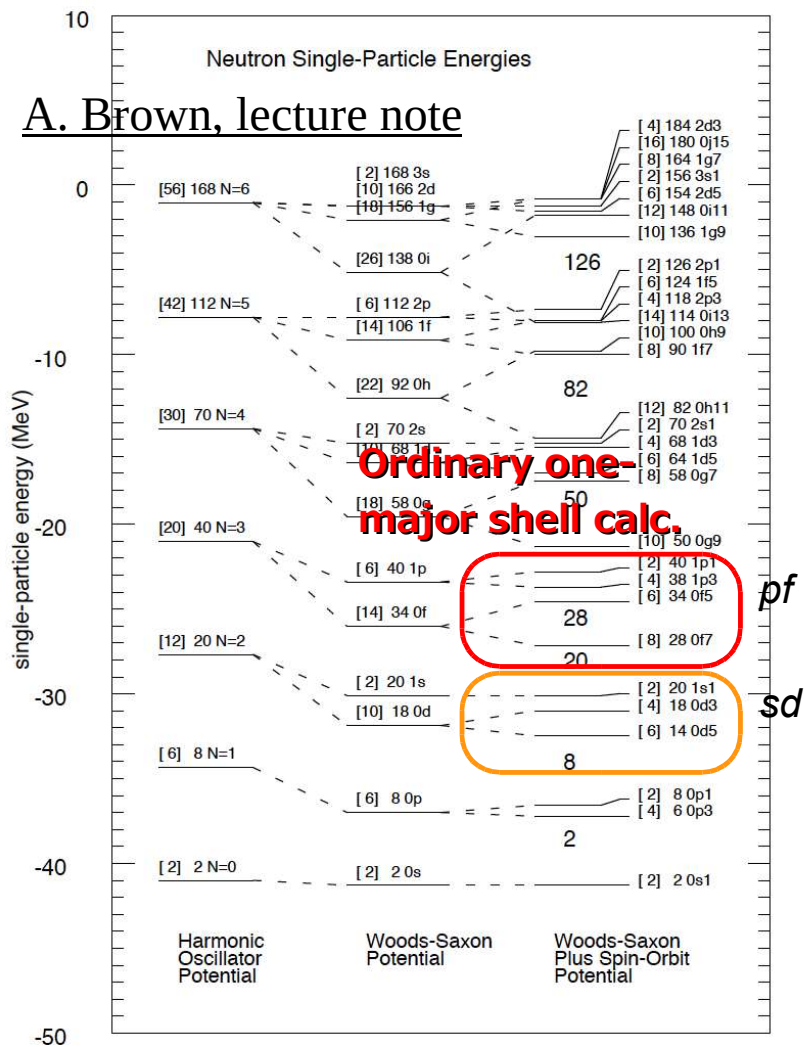
Reliability of NME values by different models

Large scale ISM calculations

Including 2 major shells (Tokyo)

One major

A. Brown, lecture note

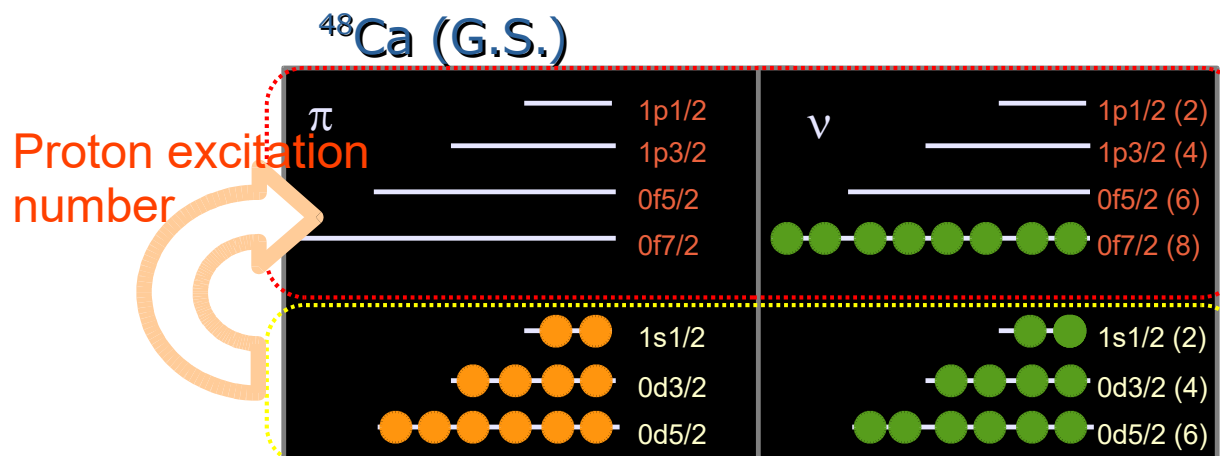


1) Adjustment of interaction for “double beta decays”

[EXPERIMENT] F. Videbaek *et al.*, NPA (1986)

2nd 0^+ state of ^{48}Ca was pointed out to be proton-excitation state

proton excitation included in 2nd 0^+ state of ^{48}Ca :



“0.22” is still too small to be pronounced as the proton-excitation state
cf.) the parity difference between the *sd*- and *pf*- orbits.

Our idea is to adjust the gap between the *sd*- and *pf*- shells
to reproduce the experimental excitation energy of 2nd 0^+ state of ^{48}Ca

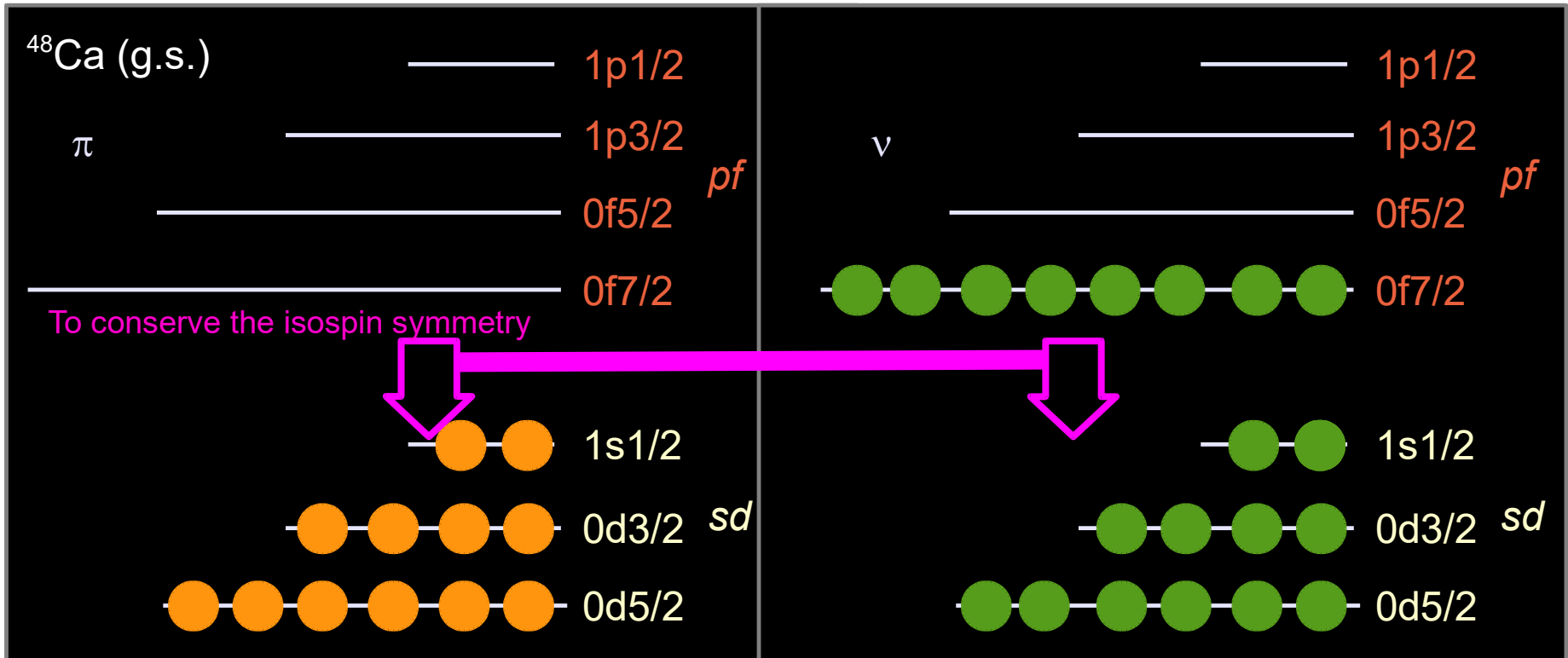
2) Shell gap

[EXPERIMENT] F. Videbaek *et al.*, NPA (1986)

2nd 0^+ state of ^{48}Ca was pointed out to be proton-excitation state

By reducing the shell gap of Ca40 about 2MeV \rightarrow 5.8 MeV

Slightly modified interaction SDPFMU-db made from SDPFMU

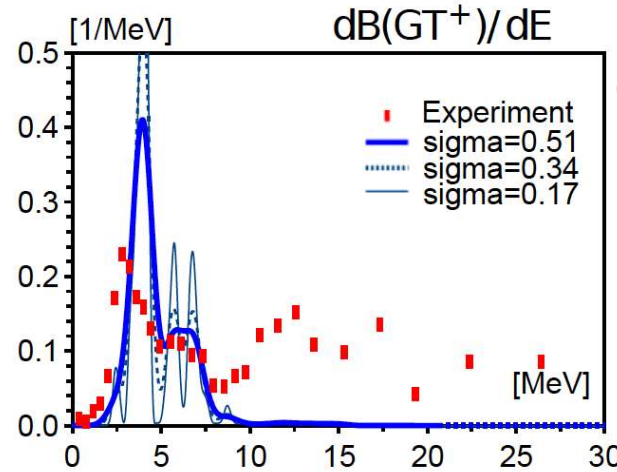
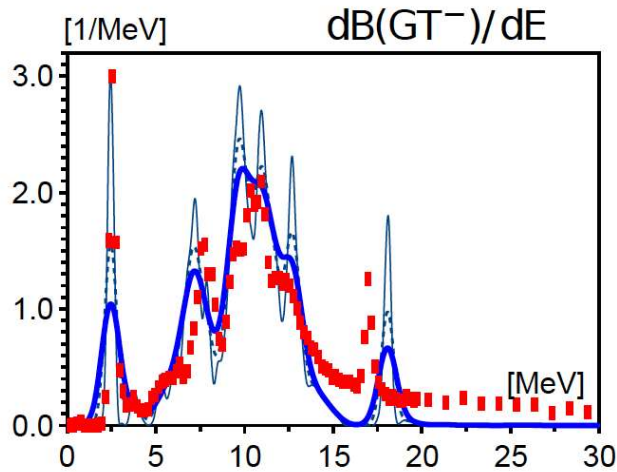


Two neutrino process

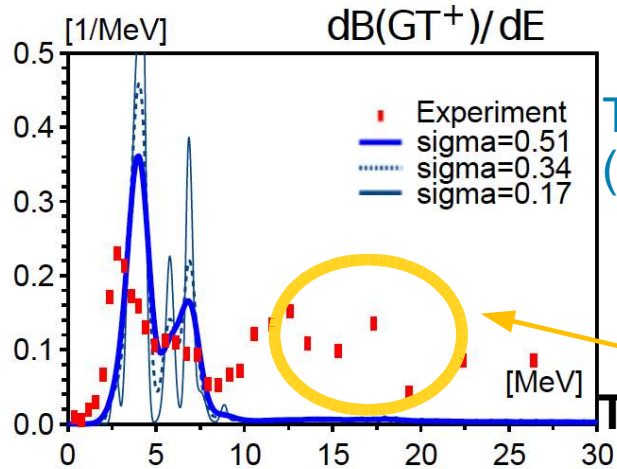
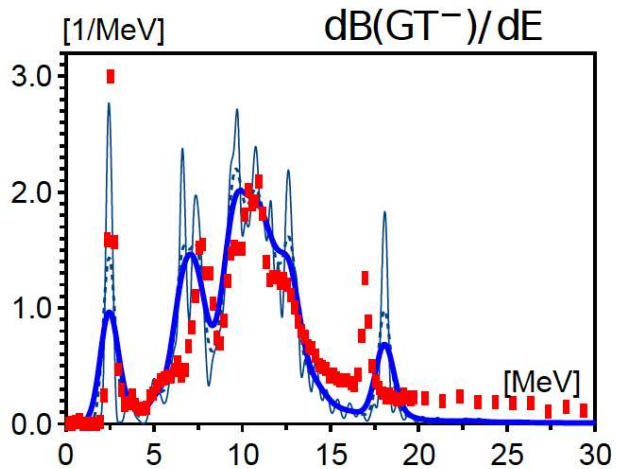
[Experiment]: Yako *et al.* PRL (2009)

Ca \rightarrow Sc

Ti \rightarrow Sc



One major shell (GXPF1A)



Two major shell (SDPF-MU)

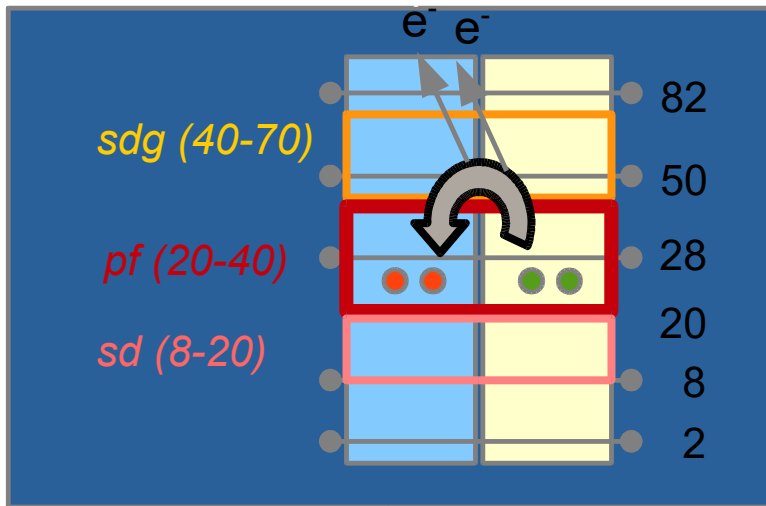
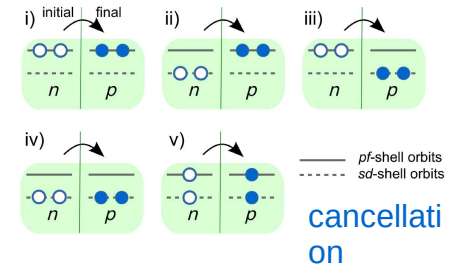
Terasaki, Phys. Rev. C 2018

Clarifies "it is IVSM"

Contribution from IVSM (isovector spin monopole) should be included in experiment. However, it is not quantitatively well known.

NME value in large model space

$$\left[T_{1/2}^{0\nu} \left(0_i^+ \rightarrow 0_f^+ \right) \right]^{-1} = G^{0\nu} |M^{0\nu}|^2 \left(\frac{\langle m_\nu \rangle}{m_e} \right)^2$$



Inclusion rate of 2nd major shell components :

^{48}Ca (22%), ^{48}Ti (33%) ***sd + pf***

^{48}Ca (~2%), ^{48}Ti (~2%) ***pf + sdg***

This result shows that

It should be necessary to take into account *sd* shell

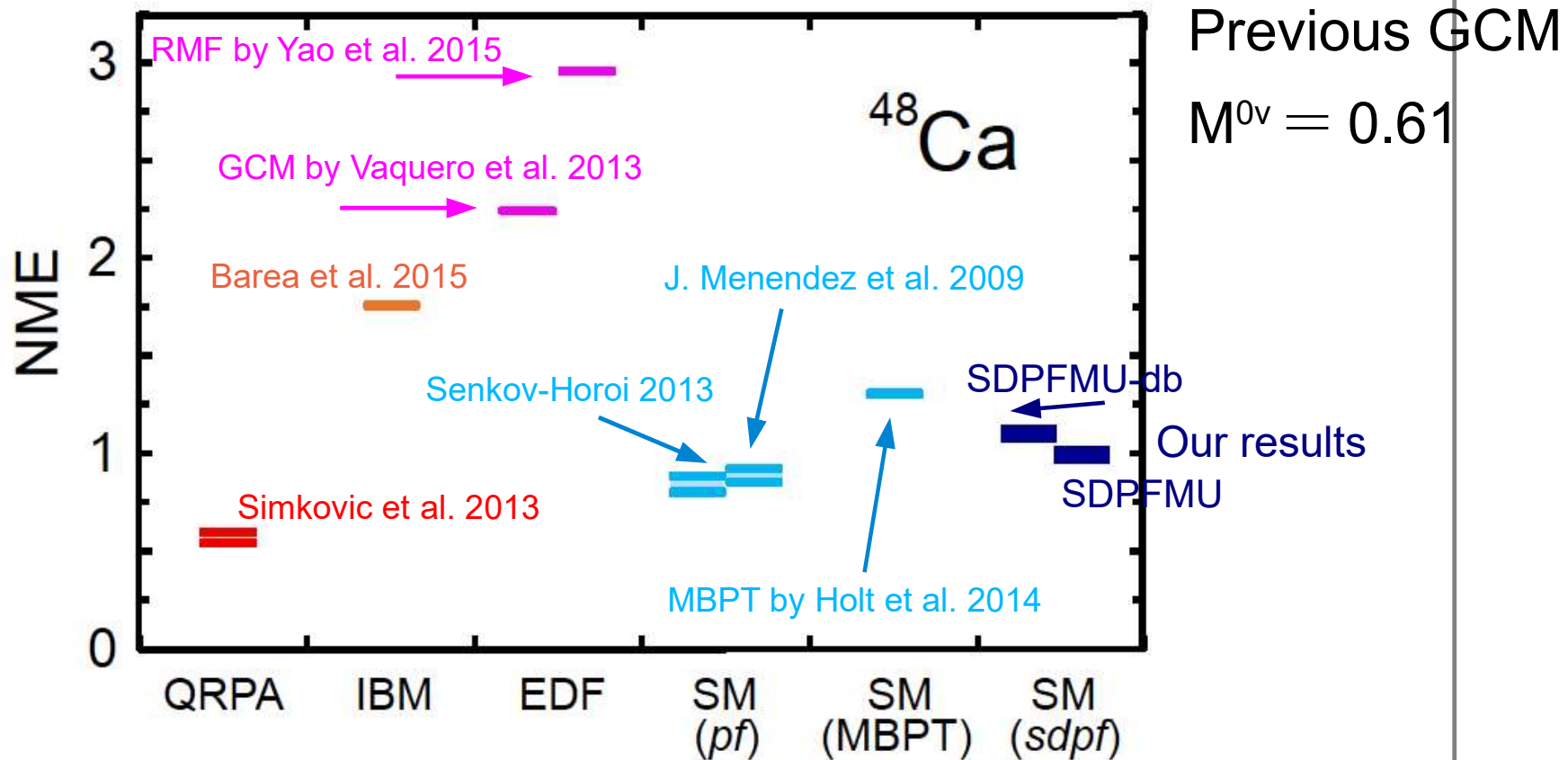
$M^{0\nu}$ (1 shell)	0.833	↓ 34.2 % increased
$M^{0\nu}$ (2 shells)	1.118	

Due to $(1/1.34)^2 \sim 0.56$,
it means that

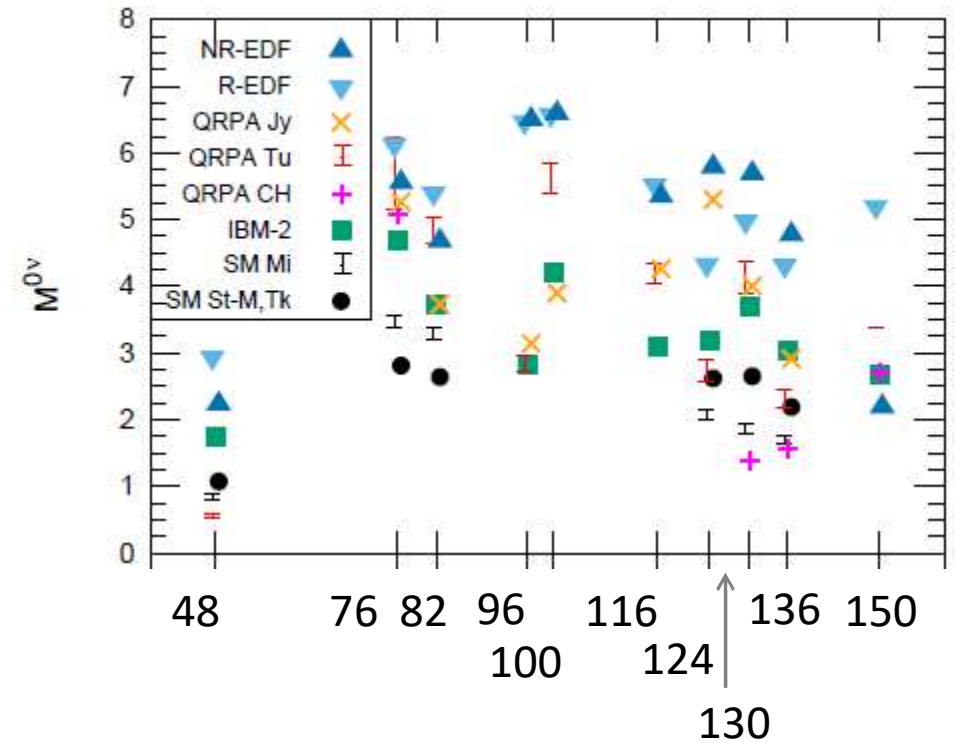
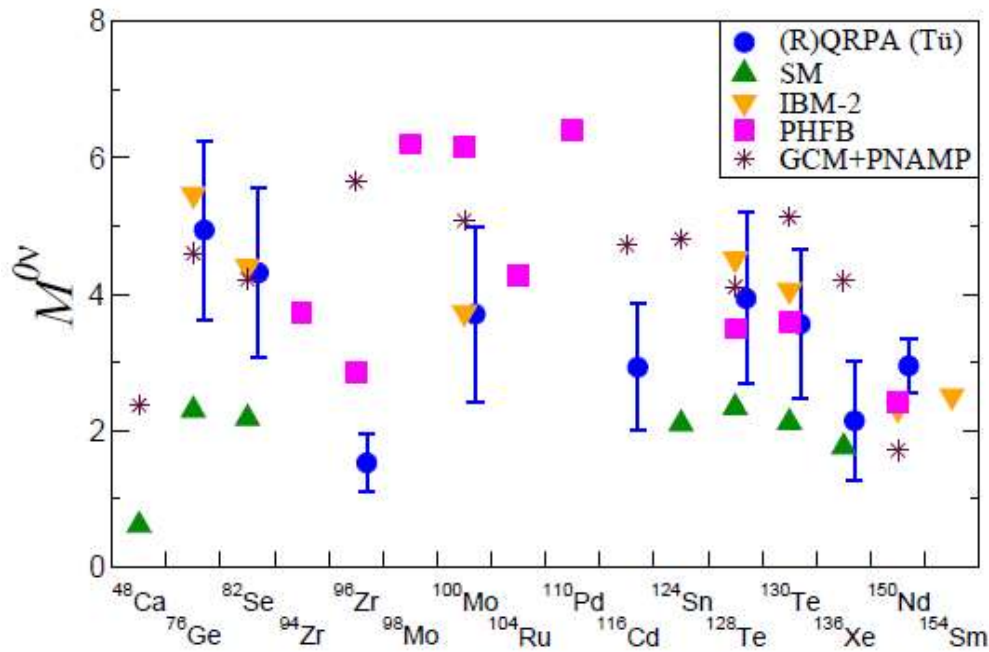
the half-life is almost halved
for the same neutrino mass.

Summary of NME for $0\nu\beta\beta$ of ^{48}Ca

Comparison of neutrinoless double beta decay NME (with ranges)



Present status for DBD candidates



A. Feassler, J. Phys.: Conf. Ser. **337**, 012065 (2012)

J. Engel and J. Menéndez, Rep. Prog. Phys. **80** (2017) 046301

There has been **no significant difference** for these 5 years.

~ 2 to 3 times difference still exists

λ mechanism

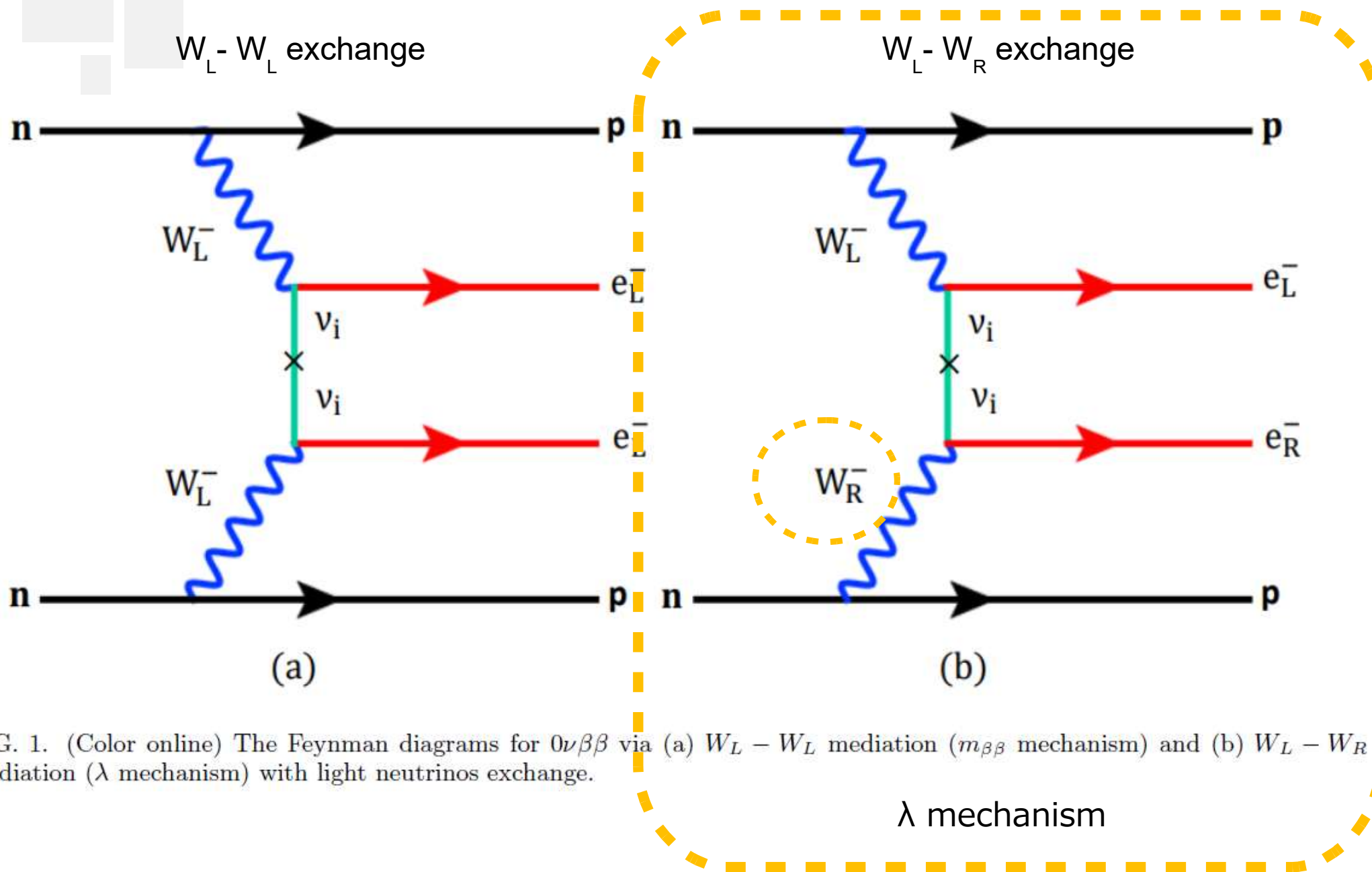
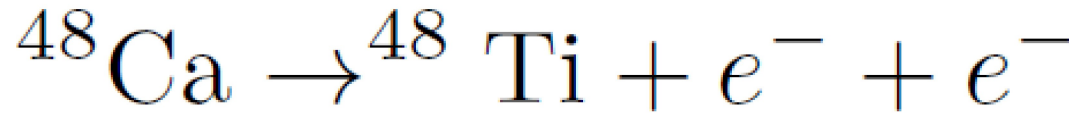


FIG. 1. (Color online) The Feynman diagrams for $0\nu\beta\beta$ via (a) $W_L - W_L$ mediation ($m_{\beta\beta}$ mechanism) and (b) $W_L - W_R$ mediation (λ mechanism) with light neutrinos exchange.

λ mechanism

Neutrinoless DBD of ^{48}Ca [Stefanik 2015]



G_{09}	10^{-9}
G_{08}	10^{-11}
G_{07}	10^{-10}
G_{06}	10^{-12}
G_{05}	10^{-13}
G_{02}	
G_{01}	10^{-14}
G_{10}	
G_{03}	
G_{11}	10^{-15}
G_{04}	

Half life (inverse)

$$[T_{1/2}^{0\nu}]^{-1} = \eta_\nu^2 C_{mm} + \eta_\lambda^2 C_{\lambda\lambda} + \eta_\nu \eta_\lambda \cos \psi C_{m\lambda}$$

usual WL-WL exchange

New

Matrix element

$$C_{mm} = g_A^4 M_\nu^2 G_{01},$$

small ~ 1/10 small ~ 1/10

$$C_{m\lambda} = -g_A^4 M_\nu M_2 (G_{03} - M_1 + G_{04})$$

$$C_{\lambda\lambda} = g_A^4 M_2^2 G_{02} + \frac{1}{9} M_1^2 G_{011} - \frac{2}{9} M_1 M_2 G_{010}$$

large ~ *10 small ~ 1/10 ~ *1

Effective lepton number violation parameters

$$\eta_\nu = \frac{m_{\beta\beta}}{m_e}, \quad \eta_\lambda = \lambda \left| \sum_{j=1}^3 m_j U_{ej} T_{ej}^* \right|,$$

$$\psi = \arg \left[\left(\sum_{j=1}^3 m_j U_{ej}^2 \right) \left(\sum_{j=1}^3 U_{ej} T_{ej}^* \right) \right]$$

accurate G_{0i} : phase space factor
($i = 1, 2, 3, \dots, 11$)

$$g_A = 1.27$$

bare

[Simkovic 2017] For Ca,

$$\eta_\nu = 2.23 \times 10^{-5}$$

$$\eta_\lambda = 2.24 \times 10^{-5}$$

Pontecorvo-Maki-Nakagawa-Sakata matrix

Calculation of nuclear matrix element

$$M_{\alpha}^{0\nu} = \langle f | \tau_{-1} \tau_{-2} \mathcal{O}_{12}^{\alpha} | i \rangle \quad \text{F, GT, T}$$

F, GT, T



$$\mathcal{O}_{12}^{GT, \omega GT, qGT} = \tau_{1-} \tau_{2-} (\sigma_1 \cdot \sigma_2) H_{GT, \omega GT, qGT}(r, E_k),$$

$$\mathcal{O}_{12}^{F, \omega F, qF} = \tau_{1-} \tau_{2-} H_{F, \omega F, qF}(r, E_k),$$

$$\mathcal{O}_{12}^{T, \omega T, qT} = \tau_{1-} \tau_{2-} S_{12} H_{T, \omega T, qT}(r, E_k),$$

$$S_{12} = 3(\sigma_1 \cdot \hat{r})(\sigma_2 \cdot \hat{r}) - (\sigma_1 \cdot \sigma_2), \quad \mathbf{r} = \mathbf{r}_1 - \mathbf{r}_2$$

$$M_{\nu} = M_{GT} - \frac{M_F}{g_A^2} + M_T,$$

$$M_{\nu\omega} = M_{\omega GT} - \frac{M_{\omega F}}{g_A^2} + M_{\omega T},$$

$$M_{1+} = M_{qGT} + 3 \frac{M_{qF}}{g_A^2} - 6 M_{qT},$$

$$M_{2-} = M_{\nu\omega} - \frac{1}{9} M_{1+}$$

$$H_{\alpha}(r, E_k) = \frac{2R}{\pi} \int_0^{\infty} \frac{f_{\alpha}(q, r) q dq}{q + E_k - (E_i + E_f)/2}$$

Included:

finite nucleon size (FNS)

higher-order currents (HOC)

Calculation of neutrino pot part

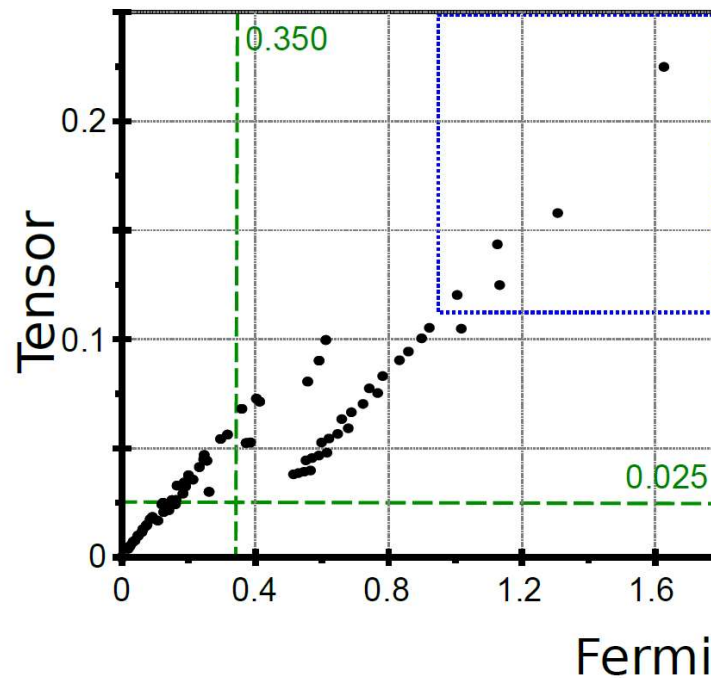
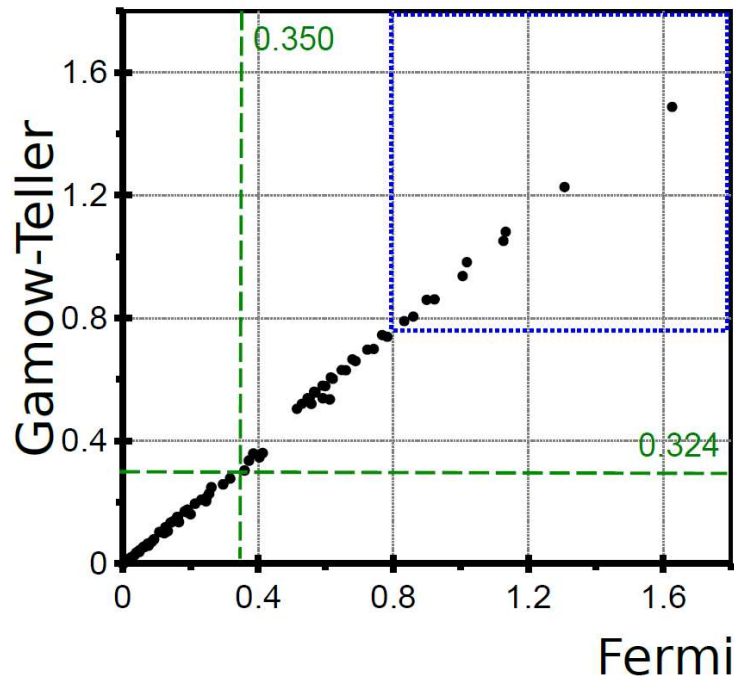
$$H_\alpha(\sqrt{2}\rho) = \frac{2R}{\pi} \int_0^\infty f_\alpha(\sqrt{2}\rho q) \frac{h_\alpha(q)}{q + \langle E \rangle} q dq$$

Closure approx.

$$\sum_{n,n',l,l'} k_{n,n',l,l'} \langle n'l' | H_\alpha(\sqrt{2}\rho) | nl \rangle$$

Top 10 amplitude

Ranking	Fermi		Gamow-Teller		Tensor	
	$(n l n' l')$	Value	$(n l n' l')$	Value	$(n l n' l')$	Value
1	(0 0 0 0)	1.626	(0 0 0 0)	1.488	(0 0 0 0)	0.2249
2	(1 0 1 0)	1.307	(1 0 1 0)	1.227	(0 0 0 1)	0.1637
3	(2 0 2 0)	1.133	(2 0 2 0)	1.081	(0 1 0 0)	
4	(0 1 0 1)	1.126	(0 1 0 1)	1.051	(1 0 1 0)	0.1579
5	(3 0 3 0)	1.018	(3 0 3 0)	0.982	(0 1 0 1)	0.1435
6	(1 1 1 1)	1.006	(1 1 1 1)	0.937	(2 0 2 0)	0.1248
7	(2 1 2 1)	0.922	(2 1 2 1)	0.861	(0 0 1 1)	0.1204
8	(0 2 0 2)	0.899	(0 2 0 2)	0.859	(1 1 0 0)	
9	(3 1 3 1)	0.859	(3 1 3 1)	0.805	(1 1 1 1)	0.1203
10	(1 2 1 2)	0.836	(1 2 1 2)	0.790	(0 1 0 2)	0.1130
					(0 2 0 1)	
					(1 0 1 1)	0.1115
					(1 1 1 0)	
					(0 0 0 2)	0.1112
					(0 2 0 0)	

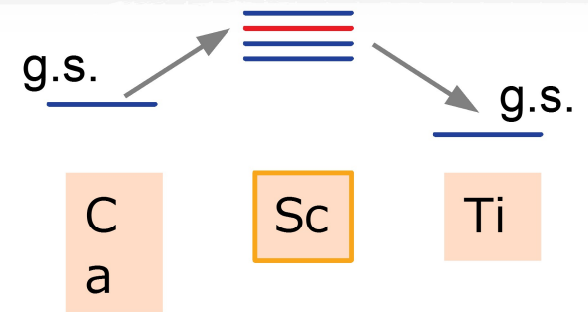


Four methods

- Closure
 - Running Closure
 - Running non-closure
- ↓
- Mixed

Running treatment

$$\sum_{J_k, J, E_k^* \leq E_c}$$



Closure:

$$H_\alpha(r) = \frac{2R}{\pi} \int_0^\infty \frac{f_\alpha(q, r) q dq}{q + \langle E \rangle}$$

Non-closure:

$$H_\alpha(r, E_k) = \frac{2R}{\pi} \int_0^\infty \frac{f_\alpha(q, r) q dq}{q + E_k - (E_i + E_f)/2}$$

Running closure

$$\bar{M}_\alpha^{0\nu}(E_c) = M_\alpha^{0\nu}(E_c) - \mathcal{M}_\alpha^{0\nu}(E_c) + \mathcal{M}_\alpha^{0\nu}$$

Running non-closure

Closure

Matrix elements [L-L type]

SRC = Short range correlation (短距離相関)

TABLE I. Nuclear matrix elements M_F , M_{GT} , M_T , M_ν for $0\nu\beta\beta$ of ^{48}Ca , calculated with GXPF1A interaction in closure, running closure, running nonclosure and mixed methods for different SRC parametrization. $\langle E \rangle = 7.72$ MeV was used for closure and running closure methods.

NME	SRC	Closure	Running closure	Running nonclosure	Mixed
M_F	None	-0.207	-0.206	-0.210	-0.211
M_F	Miller-Spencer	-0.141	-0.141	-0.143	-0.143
M_F	CD-Bonn	-0.222	-0.221	-0.226	-0.227
M_F	AV18	-0.204	-0.203	-0.207	-0.208
M_{GT}	None	0.711	0.709	0.779	0.781
M_{GT}	Miller-Spencer	0.492	0.490	0.553	0.555
M_{GT}	CD-Bonn	0.738	0.736	0.810	0.812
M_{GT}	AV18	0.675	0.673	0.745	0.747
M_T	None	-0.074	-0.072	-0.074	-0.076
M_T	Miller-Spencer	-0.076	-0.073	-0.075	-0.078
M_T	CD-Bonn	-0.076	-0.074	-0.076	-0.078
M_T	AV18	-0.077	-0.074	-0.076	-0.079
M_ν	None	0.765	0.765	0.836	0.836
M_ν	Miller-Spencer	0.504	0.505	0.566	0.565
M_ν	CD-Bonn	0.799	0.799	0.874	0.874
M_ν	AV18	0.725	0.725	0.798	0.798

Total

Matrix elements [ω type]

TABLE II. Nuclear matrix elements $M_{\omega F}$, $M_{\omega GT}$, $M_{\omega T}$, $M_{\nu\omega}$ for $0\nu\beta\beta$ of ^{48}Ca calculated with GXPF1A interaction in closure, running closure, running nonclosure and mixed methods for different SRC parametrization. $\langle E \rangle = 7.72$ MeV was used for closure and running closure methods.

NME	SRC	Closure	Running closure	Running nonclosure	Mixed
$M_{\omega F}$	None	-0.199	-0.198	-0.206	-0.207
$M_{\omega F}$	Miller-Spencer	-0.137	-0.136	-0.141	-0.142
$M_{\omega F}$	CD-Bonn	-0.212	-0.211	-0.220	-0.221
$M_{\omega F}$	AV18	-0.195	-0.194	-0.202	-0.203
$M_{\omega GT}$	None	0.66	0.659	0.766	0.767
$M_{\omega GT}$	Miller-Spencer	0.454	0.452	0.546	0.548
$M_{\omega GT}$	CD-Bonn	0.683	0.682	0.794	0.795
$M_{\omega GT}$	AV18	0.623	0.622	0.731	0.732
$M_{\omega T}$	None	-0.072	-0.069	-0.073	-0.076
$M_{\omega T}$	Miller-Spencer	-0.073	-0.070	-0.074	-0.077
$M_{\omega T}$	CD-Bonn	-0.074	-0.071	-0.075	-0.078
$M_{\omega T}$	AV18	-0.074	-0.071	-0.075	-0.078
$M_{\nu\omega}$	None	0.712	0.712	0.821	0.821
$M_{\nu\omega}$	Miller-Spencer	0.466	0.467	0.559	0.558
$M_{\nu\omega}$	CD-Bonn	0.740	0.741	0.856	0.855
$M_{\nu\omega}$	AV18	0.670	0.671	0.781	0.780

Total

The amplitude of matrix element for L-R exchange are comparable to the cases with L-L exchange.

Matrix elements [q type]

TABLE III. Nuclear matrix elements M_{qF} , M_{qGT} , M_{qT} , M_{1+} , and M_{2-} for $0\nu\beta\beta$ of ^{48}Ca calculated with GXPF1A interaction in closure, running closure, running nonclosure and mixed methods for different SRC parametrization. $\langle E \rangle = 7.72$ MeV was used for closure and running closure methods.

NME	SRC	Closure	Running closure	Running nonclosure	Mixed
M_{qF}	None	-0.102	-0.102	-0.101	-0.101
M_{qF}	Miller-Spencer	-0.082	-0.082	-0.080	-0.080
M_{qF}	CD-Bonn	-0.123	-0.122	-0.121	-0.122
M_{qF}	AV18	-0.118	-0.118	-0.117	-0.117
M_{qGT}	None	3.243	3.246	3.317	3.314
M_{qGT}	Miller-Spencer	2.681	2.684	2.751	2.748
M_{qGT}	CD-Bonn	3.554	3.557	3.709	3.706
M_{qGT}	AV18	3.423	3.426	3.502	3.499
M_{qT}	None	-0.147	-0.140	-0.143	-0.150
M_{qT}	Miller-Spencer	-0.150	-0.143	-0.146	-0.153
M_{qT}	CD-Bonn	-0.149	-0.142	-0.145	-0.153
M_{qT}	AV18	-0.150	-0.142	-0.146	-0.153
M_{1+}	None	3.937	3.898	3.989	4.028
M_{1+}	Miller-Spencer	3.430	3.389	3.480	3.521
M_{1+}	CD-Bonn	4.221	4.183	4.356	4.394
M_{1+}	AV18	4.101	4.061	4.158	4.198
M_{2-}	None	0.275	0.279	0.378	0.374
M_{2-}	Miller-Spencer	0.085	0.090	0.172	0.167
M_{2-}	CD-Bonn	0.271	0.276	0.372	0.367
M_{2-}	AV18	0.214	0.220	0.319	0.313

Total

The amplitude of matrix element for L-R exchange are relatively large compared to the cases with L-L exchange.

Spin parity decomposition

- intermediate state -

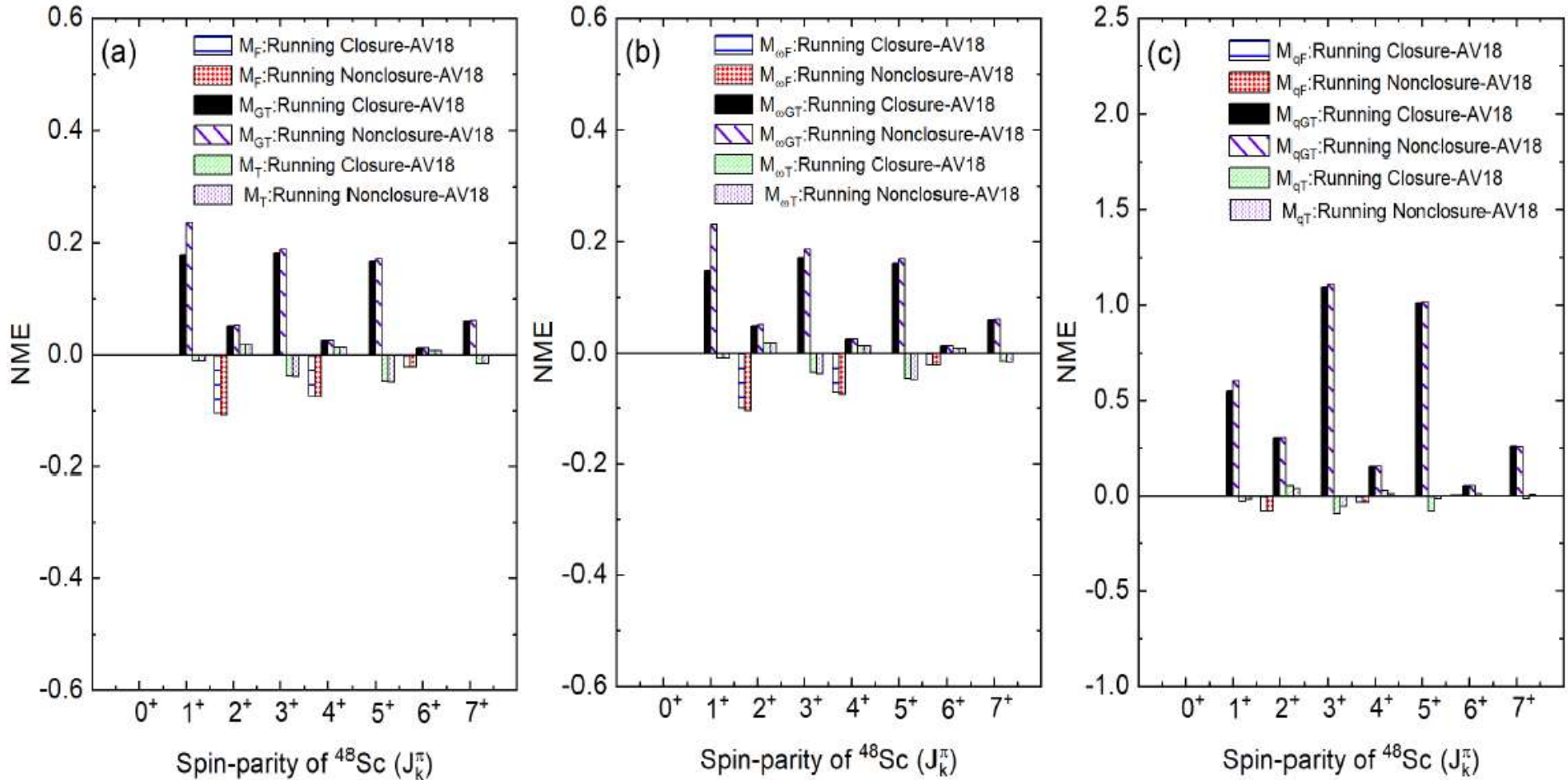
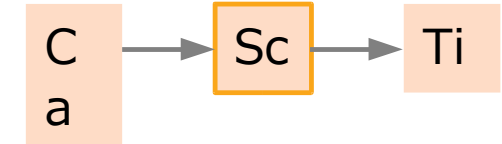


FIG. 2. (Color online) Contribution through different spin-parity of virtual intermediate states of ^{48}Sc (J_k^π) in NMEs for $m_{\beta\beta}$ and λ mechanisms of $0\nu\beta\beta$ of ^{48}Ca . Here, comparison are shown for NMEs, calculated in running closure and running nonclosure methods with GXPF1A effective interaction for AV18 SRC parametrization. $\langle E \rangle = 7.72$ MeV was used for running closure method.

Spin parity decomposition

- initial and final states -

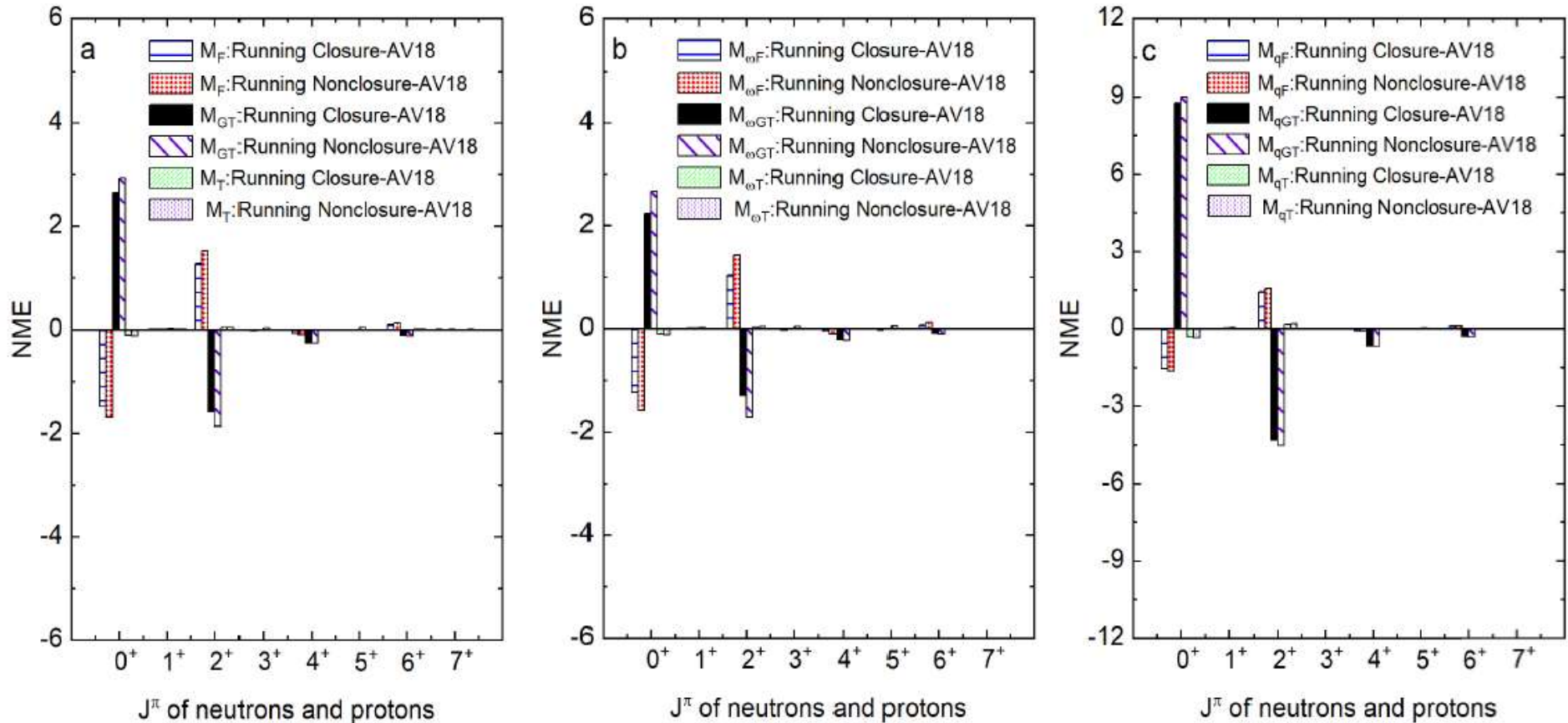
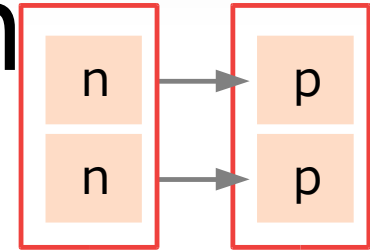
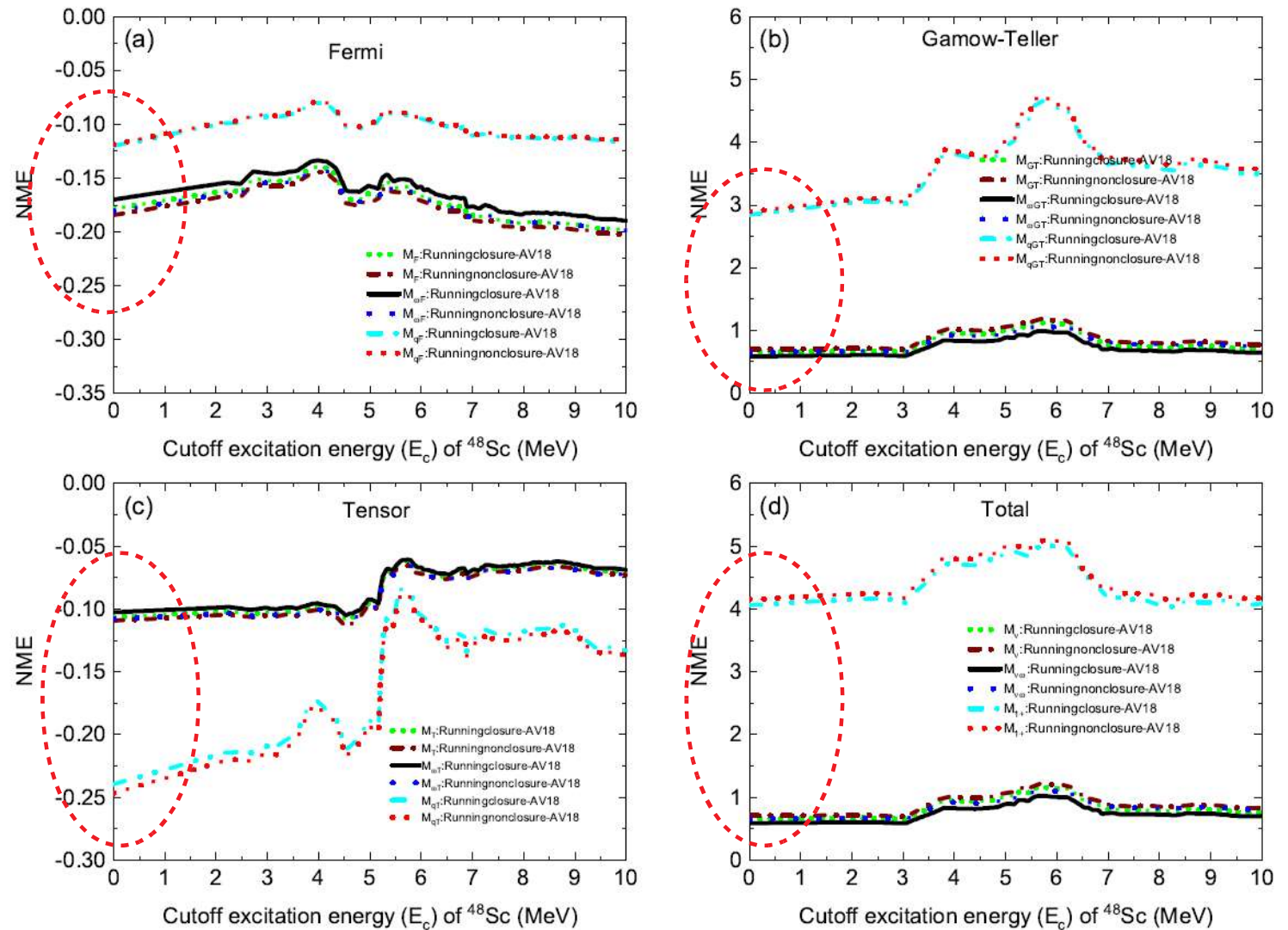


FIG. 3. (Color online) Contribution through different coupled spin-parity of two initial neutrons or two final created protons (J^π) in NMEs for $m_{\beta\beta}$ and λ mechanisms of $0\nu\beta\beta$ of ^{48}Ca . Here, comparison are shown for NMEs, calculated in running closure and running nonclosure methods with GXPF1A effective interaction for AV18 SRC parametrization. $\langle E \rangle = 7.72$ MeV was used for running closure method.

Cutoff dependence

- energy -



G.S. contribution is large

FIG. 4. (Color online) Variation of (a) Fermi (b) Gamow-Teller (c) tensor and (d) total NMEs for $0\nu\beta\beta$ ($m_{\beta\beta}$ and λ mechanisms) of ^{48}Ca with cutoff excitation energy (E_c) of states of virtual intermediate nucleus ^{48}Sc . NMEs are calculated with total GXPF1A interaction for AV18 SRC parametrization in running closure and running nonclosure methods. For running closure method, closure energy $\langle E \rangle = 7.72$ MeV was used.

Cutoff dependence

- number of states -

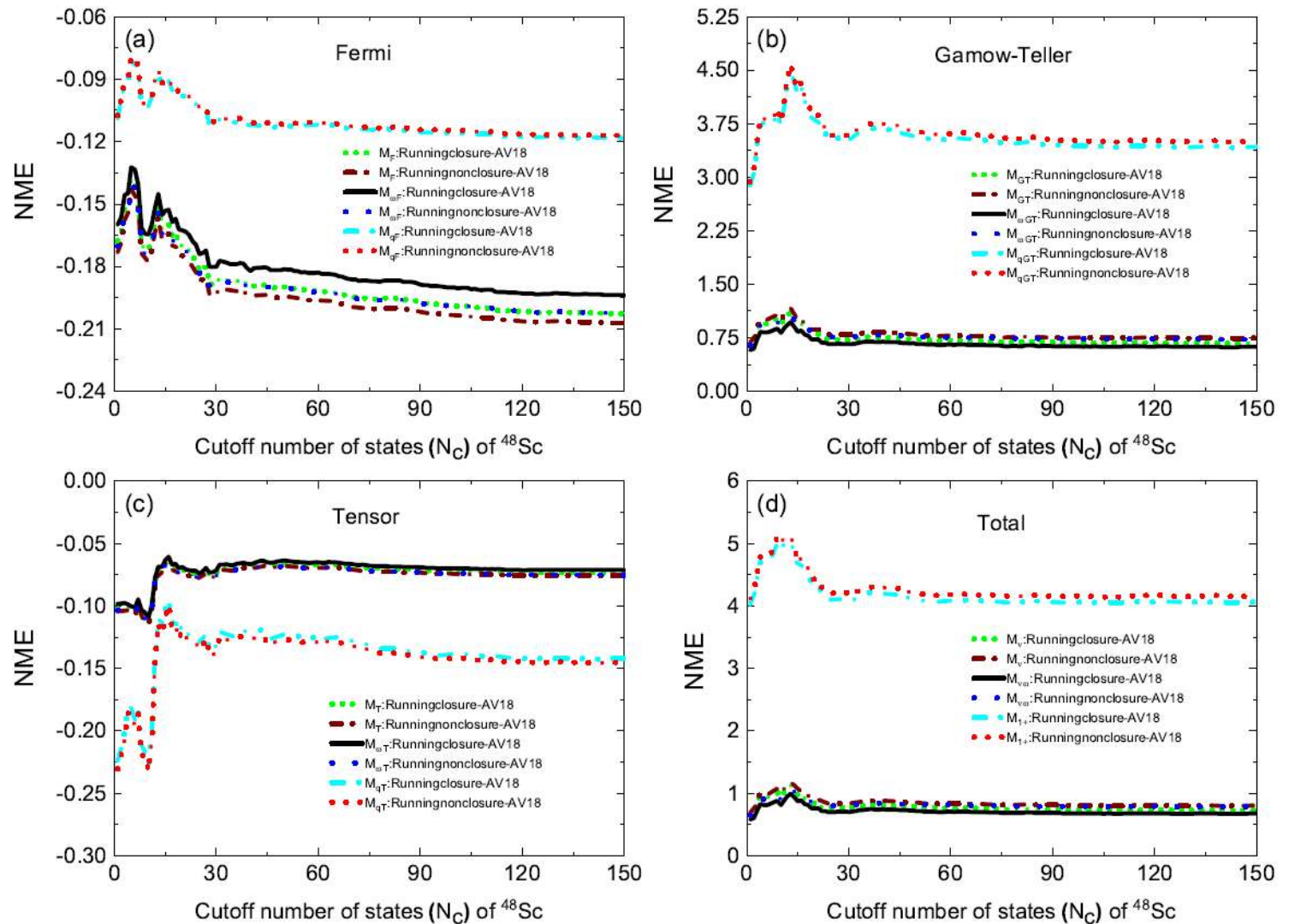


FIG. 5. (Color online) Variation of (a) Fermi (b) Gamow-Teller (c) tensor and (d) total NMEs for $0\nu\beta\beta$ ($m_{\beta\beta}$ and λ mechanisms) of ^{48}Ca with cutoff number of states (N_c) of virtual intermediate nucleus ^{48}Sc . NMEs are calculated with total GXPF1A interaction for AV18 SRC parametrization in running closure and running nonclosure methods. For running closure method, closure energy $\langle E \rangle = 7.72$ MeV was used.

Closure-energy dependence

[constant] no significant change is noticed in several settings

In closure approximation

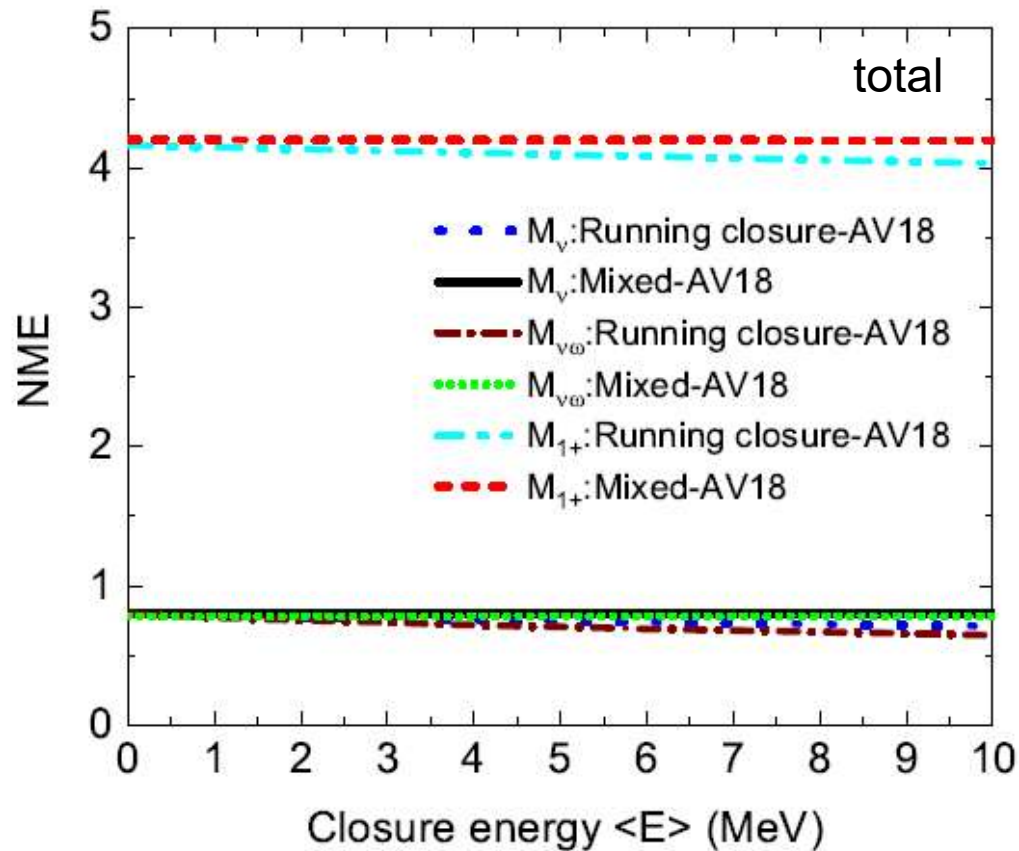


FIG. 6. (Color online) Dependence of the total NMEs for $0\nu\beta\beta$ (λ and $m_{\beta\beta}$ mechanisms) of ${}^{48}\text{Ca}$ with closure energy $\langle E \rangle$, calculated with total GXPF1A interaction for AV18 SRC parametrization in running closure and mixed methods.

Summary

$$[T_{1/2}^{0\nu}]^{-1} = \eta_\nu^2 C_{mm} + \eta_\lambda^2 C_{\lambda\lambda} + \eta_\nu \eta_\lambda \cos \psi C_{m\lambda}$$

NME	SRC	Closure	Running closure	Running nonclosure	Mixed
M_ν	None	0.765	0.765	0.836	
M_ν	Miller-Spencer	0.504	0.505	0.566	x 1
M_ν	CD-Bonn	0.799	0.799	0.874	
M_ν	AV18	0.725	0.725	0.798	
M_{1+}	None	3.937	3.898	3.989	
M_{1+}	Miller-Spencer	3.430	3.389	3.480	x 5
M_{1+}	CD-Bonn	4.221	4.183	4.356	
M_{1+}	AV18	4.101	4.061	4.158	
M_{2-}	None	0.275	0.279	0.378	
M_{2-}	Miller-Spencer	0.085	0.090	0.172	x 1/2
M_{2-}	CD-Bonn	0.271	0.276	0.372	
M_{2-}	AV18	0.214	0.220	0.319	

$$C_{mm} = g_A^4 M_\nu^2 G_{01}, \quad *1 \text{ (std)}$$

$$C_{m\lambda} = -g_A^4 M_\nu (M_{2-} G_{03} - M_{1+} G_{04})$$

$$C_{\lambda\lambda} = g_A^4 \left(M_{2-}^2 G_{02} + \frac{1}{9} M_{1+}^2 G_{011} - \frac{2}{9} M_{1+} M_{2-} G_{010} \right)$$

large ~*10 small ~1/10 ~*1

Effect should not be negligible.

$C_{\lambda\lambda}$ 1st : enlarged amplitude (*5)

$C_{\lambda\lambda}$ 2nd : comparable amplitude (*1/2)

$C_{\lambda\lambda}$ 3rd : enlarged amplitude (*2.5)

Conclusion

we have found
the large WR-WL effect

almost 2 times larger than WL-WL

$$g_V(q^2) = \frac{g_V}{\left(1 + \frac{q^2}{M_V^2}\right)^2},$$

$$g_A(q^2) = \frac{g_A}{\left(1 + \frac{q^2}{M_A^2}\right)^2},$$

$$g_M(q^2) = (\mu_p - \mu_n)g_V(q^2),$$

$$g_P(q^2) = \frac{2m_p g_A(q^2)}{(q^2 + m_\pi^2)} \left(1 - \frac{m_\pi^2}{M_A^2}\right)$$

Previous shell model calculation did not calculate/find the importance of 2nd and 3rd terms

Not calculated in
Horoi, Neascu, PRC 2018

$$f_{GT}(q, r) = \frac{j_0(qr)}{g_A^2} \left(g_A^2(q^2) - \frac{g_A(q^2)g_P(q^2)q^2}{m_N} \frac{q^2}{3} + \frac{g_P^2(q^2)q^4}{4m_N^2} \frac{q^4}{3} + \left(2 \frac{g_M^2(q^2)q^2}{4m_N^2} \frac{q^2}{3} \right) \right), \quad (15)$$

$$f_F(q, r) = g_V^2(q^2)j_0(qr), \quad (16)$$

$$f_T(q, r) = \frac{j_2(qr)}{g_A^2} \left(\frac{g_A(q^2)g_P(q^2)q^2}{m_N} \frac{q^2}{3} - \frac{g_P^2(q^2)q^4}{4m_N^2} \frac{q^4}{3} + \frac{g_M^2(q^2)q^2}{4m_N^2} \frac{q^2}{3} \right), \quad (17)$$

$$f_{\omega GT}(q, r) = \frac{q}{(q + E_k - (E_i + E_f)/2)} f_{GT}(q, r), \quad (18)$$

$$f_{\omega F}(q, r) = \frac{q}{(q + E_k - (E_i + E_f)/2)} f_F(q, r), \quad (19)$$

$$f_{\omega T}(q, r) = \frac{q}{(q + E_k - (E_i + E_f)/2)} f_T(q, r), \quad (20)$$

$$f_{qGT}(q, r) = \left(\frac{g_A^2(q^2)}{g_A^2} q + 3 \frac{g_P^2(q^2)q^5}{g_A^2 4m_N^2} + \frac{g_A(q^2)g_P(q^2)q^3}{g_A^2 m_N} \right) r j_1(q, r), \quad (21)$$

$$f_{qF}(q, r) = r g_V^2(q^2) j_1(qr) q, \quad (22)$$

$$f_{qT}(q, r) = \frac{r}{3} \left(\left(\frac{g_A^2(q^2)}{g_A^2} q - \frac{g_P(q^2)g_A(q^2)q^3}{2g_A^2 m_N} \right) j_1(qr) - \left(9 \frac{g_P^2(q^2)q^5}{2g_A^2 20m_N^2} [2j_1(qr)/3 - j_3(qr)] \right) \right),$$

Refs. for studying on this direction

λ -mechanism

D. Štefánik, R. Dvornický, F. Šimkovic, and P. Vogel, Reexamining the light neutrino exchange mechanism of the $0\nu\beta\beta$ decay with left- and right-handed leptonic and hadronic currents, *Physical Review C* **92**, 055502 (2015).

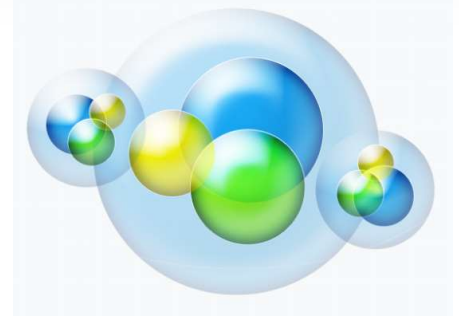
λ -mechanism (mainly by RPA calculations)

F. Šimkovic, D. Štefánik, and R. Dvornický, The λ mechanism of the $0\nu\beta\beta$ -decay, *Frontiers in Physics* **5**, 57 (2017).

Review article (e.g. hadronic current):

J. Engel and J. Menéndez, Status and future of nuclear matrix elements for neutrinoless double-beta decay: a review, *Reports on Progress in Physics* **80**, 046301 (2017).

Summary



- × ISM research [overview]
+ nuclear structure, + hadronic current, +ab-initio
→ **right-handed neutrino, right-handed W-boson**
- × Shell model calculation for DBD of Ca48
- Large scale calculation by Tokyo group -
- × Right handed weak bosons ?
- × (Right handed neutrino) --- sterile neutrinos ?